

Weather and Forecasting

Predicting 'outbreak'-level tornado counts and casualties from environmental variables --Manuscript Draft--

Manuscript Number:	WAF-D-20-0065
Full Title:	Predicting 'outbreak'-level tornado counts and casualties from environmental variables
Article Type:	Article
Corresponding Author:	Zoe Schroder Florida State University Tallahassee, FL UNITED STATES
Corresponding Author's Institution:	Florida State University
First Author:	Zoe Schroder
Order of Authors:	Zoe Schroder James B. Elsner
Abstract:	<p>Environmental variables are used routinely in forecasting when and where an outbreak of tornadoes are likely to occur, but more work is needed to understand how characteristics of severe weather outbreaks vary with the larger scale environmental factors. Here the authors demonstrate a method to quantify 'outbreak'-level tornado and casualty counts with respect to variations in large-scale environmental factors. They do this by fitting negative binomial regression models to cluster-level data to estimate the number of tornadoes and the number of casualties on days with at least ten tornadoes. Results show that a 1000 J kg^{-1} increase in CAPE corresponds to a 5% increase in the number of tornadoes and a 28% increase in the number of casualties, conditional on at least ten tornadoes, and holding the other variables constant. Further, results show that a 10 m s^{-1} increase in deep-layer bulk shear corresponds to a 13% increase in tornadoes and a 98% increase in casualties, conditional on at least ten tornadoes, and holding the other variables constant. The casualty-count model quantifies the decline in the number of casualties per year and indicates that outbreaks have a larger impact in the Southeast than elsewhere after controlling for population and geographic area.</p>

1 **Predicting ‘outbreak’-level tornado counts and casualties from**
2 **environmental variables**

3 Zoe Schroder*

4 *Department of Geography, Florida State University, Tallahassee, FL, USA, 32306*

5 James B. Elsner

6 *Florida State University, Tallahassee, FL, USA, 32306*

7 * *Corresponding author: Zoe Schroder, zms17b@my.fsu.edu*

8 * *This paper is currently under review in the journal *Weather and Forecasting*.*

ABSTRACT

9 Environmental variables are used routinely in forecasting when and where tornadoes are likely to
10 occur, but more work is needed to understand how characteristics of severe weather outbreaks vary
11 with the larger scale environmental factors. Here the authors demonstrate a method to quantify
12 ‘outbreak’-level tornado and casualty counts with respect to variations in large-scale environmental
13 factors. They do this by fitting negative binomial regression models to cluster-level data to estimate
14 the number of tornadoes and the number of casualties on days with at least ten tornadoes. Results
15 show that a 1000 J kg^{-1} increase in CAPE corresponds to a 5% increase in the number of tornadoes
16 and a 28% increase in the number of casualties, conditional on at least ten tornadoes, and holding
17 the other variables constant. Further, results show that a 10 m s^{-1} increase in deep-layer bulk shear
18 corresponds to a 13% increase in tornadoes and a 98% increase in casualties, conditional on at
19 least ten tornadoes, and holding the other variables constant. The casualty-count model quantifies
20 the decline in the number of casualties per year and indicates that outbreaks have a larger impact
21 in the Southeast than elsewhere after controlling for population and geographic area.

22 **1. Introduction**

23 Predicting characteristics (i.e, tornado counts) of severe weather outbreaks is an important and
24 challenging problem. It is important because of the potential for loss of life and property damage.
25 It is challenging because of the uncertainties associated with exactly how many and where the
26 tornadoes will occur. But progress is being made. Guidance from dynamical models help
27 forecasters outline areas of possible severe weather threats days in advance while guidance from
28 statistical models help forecasters quantify probabilities for given severe weather events (Hitchens
29 and Brooks 2014; Thompson et al. 2017; Cohen et al. 2018; Elsner and Schroder 2019; Hill et al.
30 2020). For example, Cohen et al. (2018) use a regression model to specify the probability of tornado
31 occurrence given certain environmental and storm-scale conditions (circulation above radar level,
32 rotational velocity, circulation diameter, etc). Elsner and Schroder (2019) extend this model by
33 making use of the cumulative logistic link function that predicts probabilities for each damage
34 rating using storm-relative helicity, bulk shear, convective available potential energy (CAPE), and
35 distance to a city.

36 These studies put statistical guidance for predicting severe weather outbreak characteristics on a
37 firm mathematical foundation (Cohen et al. 2018; Elsner and Schroder 2019). Room for additional
38 work in this area motivates the present study. For instance, the cumulative logistic regression
39 (Elsner and Schroder 2019) provides a distribution for the *percentage* of tornadoes within each
40 Enhanced Fujita (EF) rating category (Fujita 1981), but a model is needed to estimate the overall
41 number of tornadoes given the likelihood of at least some tornadoes.

42 Tornado outbreaks pose a risk of significant loss of life and property. Anderson-Frey and
43 Brooks (2019) consider the role environmental factors play in the number of outbreak fatalities.
44 They use self-organizing maps on the significant tornado parameter (STP) and find that more

45 damaging tornadoes (>EF3) present a higher risk for fatalities. However, they also note that both
46 deadly and non-deadly tornadoes are associated with high values of STP. Self-organizing maps are
47 useful for describing the role of environmental variables on casualties, but a statistical model is
48 needed to quantify the relationship between casualty counts and environmental factors. Here we
49 demonstrate a method to model ‘outbreak’-level tornado and casualty counts from environmental
50 conditions and predefined clusters. The model allows us to quantify the associative relationships
51 between environmental variables and tornado counts. Moreover, the approach might help extend
52 the available statistical guidance for predicting outbreak characteristics particularly when combined
53 with other models.

54 In this paper, we focus on tornado outbreaks rather than on individual tornadoes. The larger
55 space and time scales associated with the outbreak better matches our interest in the larger-scale
56 environmental factors like CAPE and shear. In what follows, we call the outbreaks ‘clusters’ as
57 is done in Schroder and Elsner (2019) because we make no attempt to associate the cluster with
58 a particular synoptic-scale system. An outbreak is defined (informally) as a group of ten or more
59 tornadoes occurring over a relatively short time scale (e.g., one day) and over a relatively limited
60 spatial domain (e.g., one to three states). Outbreaks in the United States are most frequent during
61 April, May, and June (Dixon et al. 2014; Tippett et al. 2012; Dean 2010) with most of them
62 occurring across the Central Plains and the Southeast. Outbreaks are less common in the Southeast
63 and the Southern Plains during the summer months as the jet stream migrates north taking the
64 necessary wind shear with it (Concannon et al. 2000; Gensini and Ashley 2011; Jackson and Brown
65 2009). The percentage of all U.S. tornadoes occurring in outbreaks has increased (Moore 2017;
66 Tippett et al. 2016; Elsner et al. 2015; Brooks et al. 2014).

67 This paper has two objectives: (1) demonstrate that environmental conditions prior to the oc-
68 currence of any tornadoes can be used to skillfully model the number of tornadoes in a cluster

69 containing at least ten tornadoes (tornado-count model), and (2) show that these same environ-
70 mental conditions can be used to estimate the number of casualties if the number of people in
71 harm's way is known (casualty-count model). We accomplish these objects by fitting negative bi-
72 nomial regressions to cluster-level tornado data. The data are environmental variables and tornado
73 characteristics (e.g., number of tornadoes, area of cluster, etc) on convective days (12 UTC to 12
74 UTC), when the number of tornadoes is at least ten (see Elsner and Schroder (2019)). The paper
75 is outlined as follows. The data and methods are discussed in section 2 including the mathematics
76 of a negative binomial regression. Statistics describing the response (i.e., tornado-casualty counts)
77 and environmental variables are given in section 3. The modeling results are presented in section
78 4, and a summary with conclusions are given in section 5.

79 **2. Data and methods**

80 We fit regression models to a set of tornado and reanalysis data aggregated to the level of tornado
81 clusters. Here we describe the available data and the procedures we use to aggregate values to the
82 cluster level. For our purposes, a cluster is a group of at least ten tornadoes occurring relatively
83 close to one another in both space and time between 12 UTC and 12 UTC. Ten is chosen as a
84 compromise between too few clusters leading to greater uncertainty and too many clusters leading
85 to excessive time required to fit the models (Elsner and Schroder 2019). It is also the number
86 that is sometimes used formally to define an outbreak. The number of tornadoes in each cluster is
87 the response variable in the tornado-count regression model, and the number of casualties is the
88 response variable in the casualty-count regression model. Explanatory variables include outbreak
89 size and location as well as environmental variables from reanalysis data representing conditions
90 before the occurrence of the first tornado in the cluster.

91 *a. Tornado clusters*

92 First, we extract the date, time, genesis location, and magnitude of all tornado reports between
93 1994 and 2018 from the Storm Prediction Center [SPC] ([https://www.spc.noaa.gov/gis/
94 svrgis/](https://www.spc.noaa.gov/gis/svrgis/)). We choose 1994 as the start year because it is the first year of the extensive use of the
95 WSR-88D Radar (Heiss et al. 1990). Each row in the dataset contains information at the individual
96 tornado level. In total, there are 30 497 tornado reports during this period. The geographic
97 coordinates for each genesis location are converted to Lambert conic conformal coordinates, where
98 the projection is centered on 107° W longitude.

99 Next, we assign to each tornado a cluster identification number based on the space and time
100 differences between genesis locations. Two tornadoes are assigned the same cluster identification
101 number if they occur close together in space and time (e.g., 1 km and 1 h). When the difference
102 between individual tornadoes and existing clusters surpasses 50 000 s (~ 14 h), the clustering
103 ends. The space-time differences have units of seconds because we divide the spatial distance
104 by 15 m s^{-1} to account for the average speed of tornado-producing storms. We note that this
105 speed is commensurate with the magnitude of the steering-level wind field across the clusters.
106 The clustering is identical to that used in Elsner and Schroder (2019) who developed a cumulative
107 logistic model to the damage scale at the individual tornado level. Additional details on the
108 procedure, as well as a comparison of the identified clusters to well-known outbreaks, are available
109 in Schroder and Elsner (2019).

110 We keep only clusters having at least ten tornadoes occurring within the same convective day,
111 which results in 768 clusters with a total of 17 069 tornadoes. A convective day is defined as a
112 24-hour period beginning at 1200 UTC (Doswell et al. 2006). The average number of tornadoes
113 (for clusters with at least ten tornadoes) is 22 tornadoes and the maximum is 173 tornadoes (April

114 27, 2011). There are 80 clusters with exactly ten tornadoes. Each cluster varies by area and by
115 where it occurs (Fig. 1). The cluster area is defined by the minimum convex hull (black polygon)
116 that includes all the tornado genesis locations. The July 19, 1994 cluster with nine tornadoes over
117 northern Iowa and one over northwest Wisconsin had an area of 33 359 km² and lasted about four
118 hours. The April 27, 2011 cluster had 173 tornadoes spread over more than a dozen states and
119 had an area of 1 064 337 km² with tornadoes occurring throughout the 24-h period (12-UTC to
120 12-UTC).

121 For each cluster we sum the number of injuries and deaths across all tornadoes to get the cluster-
122 level number of casualties (sum of injuries and fatalities). Further we estimate the population within
123 the cluster area and the geographic center of the cluster. Population are U.S. Census estimates in
124 cities with at least 40,000 people (Steiner 2019). Population is used as an explanatory variable in
125 place of cluster area when the number of casualties is the response variable.

126 *b. Environmental variables*

127 Large-scale environmental conditions for producing tornadoes are well studied and include large
128 magnitudes of convective available potential energy, bulk shear, and weak convective inhibition
129 (Brooks et al. 1994; Rasmussen and Blanchard 1998; Thompson et al. 2003; Shafer and Doswell
130 2011; Doswell et al. 2006). We obtain variables associated with these environmental condi-
131 tions from the National Centers for Atmospheric Research’s North American Regional Reanalysis
132 (NARR), which is supported by the National Centers for Environmental Prediction (Mesinger et al.
133 2006). Each variable has numeric values given on a 32-km raster grid with the values available
134 in three-hour increments starting at 00 UTC. We note that in the severe weather literature these
135 environmental variables are called ‘parameters’. However here, since we employ statistical mod-
136 els, we prefer to call them variables to be consistent with the statistical literature where the word

137 ‘parameter’ denotes unknown model coefficients and moments of statistical distributions (e.g., the
138 mean).

139 We select environmental variables at the nearest three-hour time *prior* to the occurrence of the
140 first tornado in the cluster. For example, if the first tornado in a cluster occurs at 16:30 UTC we
141 use the environmental variables given at 15 UTC. This selection criteria results in a sample of the
142 environment that is less contaminated by the deep convection itself but at a cost that underestimates
143 the severity in cases where rapid increases in conditions favoring tornadoes occur. We note that
144 about 60% of all clusters have the initial tornado occurring between 18 and 00 UTC (Table 1). We
145 also note that there are more tornadoes in clusters when the first tornado occurs between 15 and 18
146 UTC on average.

147 The environmental variables we consider include convective available potential energy (CAPE)
148 and convective inhibition (CIN) as computed using the near-surface layer (0 to 180 mb above the
149 ground level) consistent with Allen et al. (2015b). We also include deep (1000 to 500 mb) and
150 shallow (1000 to 850 mb) layer bulk shears (DLBS, SLBS) computed as the square root of the sum
151 of the squared differences between the u and v wind components at the respective levels consistent
152 with Tippett et al. (2012). Climate researchers use these NARR variables as proxies for the more
153 traditional variables used in real-time forecasting of severe weather (Allen et al. 2015b; Moore
154 et al. 2016; Tippett et al. 2012). We take the highest (lowest for CIN) value across the grid of
155 values within the area defined by the cluster’s convex hull. This is done to capture environmental
156 conditions that represent the unadulterated pre-tornado environment. In contrast, the mean (or
157 median) value is influenced by conditions throughout the domain including earlier occurring non-
158 tornado-producing convection. Histograms of the maximums (not shown) provide no evidence of
159 outlier behavior.

Storm-relative helicity is not used because it is correlated with DLBS and SLBS (Table 2). Likewise dew-point temperature and specific humidity are not used because of their relatively high correlation with CAPE. Further we do not use composite variables including the significant tornado parameter (STP) and the supercell composite parameter (SCP). STP, for example, is the product of variables including CAPE, storm-relative helicity, CIN, and lifted condensation level (LCL) height. A moderate value of STP can result from either high CAPE and low shear or low CAPE and high shear environments holding the other variables constant. Here we separate this composite relationship to examine the direct relationships between CAPE and shear on tornado activity at the scale of outbreaks.

c. Negative binomial regression

With the cluster as our unit of analysis, we fit a series of regression models to the data having the form

$$T \sim \text{NegBin}(\hat{\mu}, n)$$

$$\ln(\hat{\mu}) = \beta_0 + \beta_A A + \beta_\phi \phi + \beta_\lambda \lambda + \beta_Y Y + \beta_{CAPE} \text{CAPE} + \beta_{CIN} \text{CIN} + \beta_{DLBS} \text{DLBS} + \beta_{SLBS} \text{SLBS}, \quad (1)$$

where the number of tornadoes (T) is the dependent variable that is assumed to be adequately described by a negative binomial distribution (NegBin) with a rate parameter μ and a size parameter n (Hilbe 2011). The natural logarithm of the rate parameter is linearly related to cluster area (A), cluster center location [latitude (ϕ) and longitude (λ)], year (Y) and the four environmental variables (CAPE, CIN, DLBS, and SLBS). The model is fit using the method of maximum likelihoods carried out in the call to the `glm.nb` function from MASS package in R (Venables and Ripley 2002). We do the same for the initial casualty-count model, but we replace cluster area with population (P). We simplify the initial models by single-term deletions as described in §4.

3. Descriptive statistics

The number of clusters decreases exponentially with an increasing number of tornadoes per cluster (Fig. 2). There are 80 clusters with ten tornadoes but only ten clusters with 30 tornadoes. The right tail of the count distribution is long with the April 27, 2011 cluster having 173 tornadoes [47 (6%) of the clusters have more than 50 tornadoes and are not shown]. However more clusters have 20 or 21 tornadoes than expected from a simple decay function. This deviation is unlikely the result of physical processes, and it appears too large to be sampling variability. The distribution of casualties is also skewed toward many clusters having only a few casualties and a few have many. Thirty-six percent of all clusters (275) are without a casualty and 56% of the clusters have fewer than four casualties.

There is a seasonality to the chance of at least one tornado cluster (Fig. 3). The empirical seven-day probability of at least one cluster is between 20 and 30% for much of the year except between the middle of March and early July (Fig. 3A). The probabilities approach 80% between mid and late May. The number of tornadoes per cluster is less variable ranging between about 10 and 35 tornadoes per week with no strong seasonality although clusters during July and August tend to have somewhat fewer tornadoes (Fig. 3B). The casualty rate, defined as the number of casualties per 100,000 people within the cluster area, has a distinct seasonality with rates being highest between March to April and August to September (Fig. 3C).

Across the 768 clusters the mean of the maximum values of CAPE is $2\,225\text{ J kg}^{-1}$ and the mean of the minimum values of CIN is -114 J kg^{-1} (Table 3). The maximum deep-layer bulk shear values range from 5.6 to 47.9 m s^{-1} . Cluster areas range from 361 to $1\,064\,337\text{ km}^2$ with an average of $167\,990\text{ km}^2$.

4. Results

a. A model for the number of tornadoes

First, we fit a negative binomial regression to the cluster-level tornado counts using the explanatory variables given in Table 3. This is our tornado-count model. We divide the cluster area by 10 million so it has units of 100 km^2 . We divide CAPE by 1000 so it has units of 1000 J kg^{-1} and we divide CIN by 100 so it has units of 100 J kg^{-1} . This simplifies interpretation of the model coefficients, but does not affect the goodness of fit.

All terms have signs on the coefficient that are physically reasonable (Table 4). The number of tornadoes in a cluster increases with cluster area, CAPE, and bulk shear (deep and shallow layers) and increases for decreasing CIN (i.e., less inhibition) as expected. The significance of the variable in statistically explaining tornado counts is assessed by the corresponding z -value given as the ratio of the coefficient estimate to its standard error (S.E.). We reject the null hypothesis that a particular variable has no explanatory power if its corresponding p -value is less than .01. Here we fail to reject the null hypothesis for the variables latitude, longitude, and year, which indicates that these non-physical variables have a relatively small impact on tornado counts relative to the physical variables given the data and the model. In particular, there is no significant upward or downward trend over time in the number of tornadoes in these clusters. The only physical variable that is not statistically significant is CIN. We remove all statistically insignificant variables before fitting a final model.

All variables in the final model are significant although the coefficients have changed a bit relative to the initial model. The in-sample correlation between the observed counts and predicted rates is .59 [(0.54, 0.64), 95% uncertainty interval (UI)] (Fig. 4). We find that the model is not improved by using the average values of the same environmental variables. The model statistically explains

225 almost 60% of the variation in cluster-level tornado counts but tends to over predict the number of
 226 tornadoes for smaller clusters and slightly under predict the number of tornadoes for larger clusters.
 227 The mean absolute error between the observed counts and expected rates is 8.6 tornadoes or 5.2%
 228 of the range in observed counts and 9.3% of the range in predicted rates. The out-of-sample
 229 errors are quite similar due to the large sample size (768 clusters). A hold-one-out cross validation
 230 exercise (Elsner and Schmertmann 1994) results in an out-of-sample correlation of .58 and a mean
 231 absolute error of 8.6 tornadoes. The lag-1 temporal autocorrelation in cluster-level tornado counts
 232 is .13.

233 The value of β_0 (Table 4) is the regression estimate when all variables in the model are evaluated at
 234 zero. The effect size for a given explanatory variable is given by the magnitude of its corresponding
 235 coefficient. The coefficient is expressed as the difference in the logarithm of the expected tornado
 236 counts for a unit increase in the explanatory variable holding the other variables constant. For
 237 example, the scaled units of CAPE are 1000 J kg^{-1} . An increase in CAPE of 1000 J kg^{-1} results in
 238 a $(\exp(.0459) - 1) \times 100\% = 4.7\%$ increase in the expected number of tornadoes, conditional on at
 239 least ten tornadoes. Continuing, units of deep-layer bulk shear are 10 m s^{-1} so an increase in shear
 240 of 10 m s^{-1} results in a 13% increase in the expected number of tornadoes. A similar increase in
 241 shallow-layer bulk shear results in a 11.1% increase in the number of tornadoes.

242 Changes to the expected number of tornadoes given changes in the environmental variables
 243 have a large impact on the probability distribution of counts conditional on the cluster area. The
 244 negative binomial distribution for the number of tornadoes T with an expected number of tornadoes
 245 \bar{T} (obtained from the regression model) has a probability density

$$\Pr(T = k) = \frac{\Gamma(r+k)}{k! \Gamma(r)} \left(\frac{r}{r+\bar{T}} \right)^r \left(\frac{\bar{T}}{r+\bar{T}} \right)^k \quad \text{for } k = 10, 11, 12, \dots, \quad (2)$$

246 where $r = 1/n$ and $\Gamma(z) = \int_0^\infty x^{z-1} e^{-x} dx$ is the gamma function.

247 For example, on April 12, 2020 the 12 UTC guidance from the SPC convective outlook defined
248 an area with a 10% chance of at least one tornado occurring within 40 km of any location (10%
249 tornado risk). The area of the polygon was approximately 400 000 km² (much larger than the
250 average cluster area) centered on Mississippi. With an area of that size, the model estimates the
251 probability of at least 30 tornadoes for a range of deep-layer shear values and conditional on the
252 amount of CAPE while holding shallow-layer shear at an average value (Fig. 5). Given an average
253 amount of shallow-layer shear, a deep-layer shear of 10 m s⁻¹ and low CAPE (5th percentile value),
254 the model predicts a 17% [9, 26%, UI] chance of at least 30 tornadoes (given a cluster with at least
255 ten tornadoes). In contrast, given a deep-layer shear of 40 m s⁻¹ and high CAPE (95th percentile
256 value), the model predicts a 65% [(56, 71%), UI] chance of at least 30 tornadoes. There were more
257 than 100 tornadoes on that day.

258 The model quantifies the empirical relationship between CAPE and, independently, shear in
259 terms of a probability distribution on the number of tornadoes. It predicts the expected count
260 given values for the explanatory variables. The negative binomial distribution uses the model's
261 predicted count and the size parameter to generate a distribution of probabilities. For example, the
262 model gives predicted probabilities across a range of CAPE and deep-layer shear values (holding
263 shallow-layer shear at its mean value) that provides a picture of the relationship (Fig. 6). The
264 predicted probabilities of at least 30 tornadoes given an outbreak covering an area of 400 000 km²
265 increase from low values of both CAPE and shear to high values of both CAPE and shear.

266 *b. A model for the number of casualties*

267 Next we fit a negative binomial regression to the cluster-level casualty counts (direct injuries and
268 deaths) using the same explanatory variables (Table 3) with the exceptions that population (scaled
269 by 100,000 residents) replaces cluster area and C (casualty count) replaces T (tornado count) as

270 the dependent variable. This is our casualty-count model. We find that CIN is the only variable
271 not significant in the initial model (Table 5). We remove it before fitting a final model.

272 The in-sample correlation between the observed casualty counts and predicted rates is .43 [($.37$,
273 $.48$), 95% UI] (Fig. 7). The mean absolute error between the observed counts and expected rates
274 is 39 casualties or 1.3% of the range in observed counts and 3.4% of the range in predicted rates.
275 The out-of-sample correlation is .36 and the mean absolute error is 40 casualties. The skill is
276 lower than the skill of the tornado-count model as there is additional uncertainty associated with
277 the number of casualties given a tornado.

278 As expected from the tornado-count model, the number of casualties resulting from a cluster of
279 tornadoes increases with CAPE and with the two bulk shear variables (Table 5) which is consistent
280 with Anderson-Frey and Brooks (2019). Holding all other variables constant, an increase in CAPE
281 of 1000 J kg^{-1} results in a 28% increase in the expected number of casualties. An increase in
282 deep-layer bulk shear of 10 m s^{-1} results in a 98% increase in the expected number of casualties per
283 cluster and a similar increase in shallow-layer bulk shear results in a 76% increase in the expected
284 number of casualties per cluster, conditional on at least ten tornadoes. There is also a significant
285 downward trend (negative value for the β_Y coefficient) in the number of casualties at a rate of 3.6%
286 per year. This is very likely the result of improvements made by the National Weather Service
287 in warning coordination and dissemination leading to better awareness especially for these large
288 outbreak events.

289 Also as expected the number of people in harm's way is a significant predictor for the cluster-level
290 casualty count. The relationship between population and number of casualties is quantified at the
291 tornado-level in Elsner et al. (2018) and Fricker et al. (2017) so we expect it to hold at the cluster
292 level. Here, we are able to compare the influence of shear and CAPE on the probability of casualties
293 as modulated by population (Fig. 8). Model results are shown for three levels of population. The

294 probability of a large number of casualties increases with increasing shear and increasing CAPE,
295 while keeping the other variables at their mean values and year at 2018.

296 Importantly, we also find that where the cluster occurs has a significant influence on the number
297 of casualties consistent with other studies (Ashley and Strader 2016; Fricker and Elsner 2019).
298 For every one degree north latitude the casualty rate decreases by 5.5% and for every one degree
299 east longitude the casualty rate increases by 2.9%. Thus, cluster-level casualties are highest over
300 the Southeast. This effect is independent of the number of tornadoes since location was not a
301 significant factor in the tornado-count model. The result is also independent of the number of
302 people in harm's way since population is included as an exploratory variable in the model.

303 To visualize the difference of the combined effects of latitude and longitude on the difference in
304 the probability of many casualties, we plot modeled casualty probabilities (at least 25) as a function
305 of CAPE and deep-layer shear for two *hypothetical* outbreaks that are the same in every way except
306 one outbreak is center on Sioux City, Iowa, and the other is centered on Birmingham, Alabama
307 (Fig. 9). The modeled probabilities are lowest (around 5%) for low CAPE and shear values and
308 highest (above 30%) for high CAPE and shear values. The difference in modeled probabilities
309 across these two locations peaks at about +12 percentage points for high CAPE and high shear
310 regimes when the outbreak is centered on Birmingham.

311 **5. Summary and conclusions**

312 Forecasting characteristics of severe weather outbreaks (e.g., tornado and casualty counts) is
313 challenging but important. Forecasters use a combination of numerical weather prediction and
314 empirical guidance to outline areas of severe convective weather. Here we demonstrate a statistical
315 regression model that can take advantage of the large sample of independent tornado 'outbreaks'
316 as a way to statistically explain the number of tornadoes and the number of casualties in a cluster

317 of at least ten tornadoes. Much more work is needed to adopt the modeling strategy in an
318 operational forecast setting. For use in forecasts, future work should distinguish between tornadic
319 and nontornadic outbreaks and consider using forecast data as opposed to NARR.

320 Here we fit negative binomial regressions to observed data aggregated to the level of tornado
321 clusters where a cluster is a space-time group of at least ten tornadoes occurring between 12
322 UTC and 12 UTC over the period 1994–2018. The number of tornadoes in each cluster is the
323 response variable in the tornado-count model, and the number of casualties (deaths plus injuries)
324 is the response variable in the casualty-count model. Environmental explanatory variables for the
325 models are extracted from reanalysis data representing conditions before the occurrence of the first
326 tornado in the cluster consistent with Schroder and Elsner (2019). Additional explanatory variables
327 include cluster area, population, location, and year.

328 The predicted tornado rates, conditional on there being at least ten tornadoes, explain 59% of the
329 observed tornado counts in-sample, and the predicted casualty rates explain 43% of the observed
330 casualty counts in-sample. Because of the large sample size, the out-of-sample skill is lower but
331 still useful. The models show that a 1000 J kg^{-1} increase in CAPE results in a 4.7% increase in
332 the expected number of tornadoes conditional on at least ten tornadoes and a 28% increase in the
333 expected number of casualties, holding the other variables constant consistent with recent work
334 (Anderson-Frey and Brooks 2019). The models further show that a 10 m s^{-1} increase in deep-layer
335 bulk shear results in a 13% increase in the expected number of tornadoes and a 98% increase in
336 the expected number of casualties, holding the other variables constant consistent with recent work
337 (Anderson-Frey and Brooks 2019). The casualty-count model also shows a significant decline in
338 the number of casualties at a rate of 3.6% per year. Casualty rates depend on where the outbreak
339 occurs with more deaths and injuries, on average, over the Southeast, controlling for the other
340 variables; a result that is consistent with the recent work of Fricker and Elsner (2019).

341 Some of the unexplained variability in cluster-level tornado counts (and casualty counts) arises
342 from the uncertainty associated with the preferred storm mode and the evolution of meso-scale
343 convective systems, neither of which are captured by a single maximum value in the variable space
344 of CAPE and shear. The counts are also limited by the quality of the NARR data. The NARR
345 tends to unrealistically favor tornado environments during specific convective setups (Gensini and
346 Ashley 2011; Gensini et al. 2014; Allen et al. 2015a). Also, outbreaks associated with tropical
347 cyclones likely add a bit of noise to both models since the number of tornadoes is sensitive to the
348 extent and location of convective bursts within overall evolution of the land-falling storm.

349 The casualty-count model would be improved by including a skillful prediction of the number
350 of tornadoes. Indeed in a perfect-prognostic setting, where we know the number of tornadoes in
351 the outbreak, the out-of-sample correlation between the observed number of casualties and the
352 modeled estimated rate of casualties increases to .79. Further, although our approach to extracting
353 signal from noise in the tornado dataset is sound, exclusive focus on clusters with at least ten
354 tornadoes is a type of selection bias meaning that the sample of data used to fit the model does not
355 represent the population of all outbreaks, which limits what we can say in general about the effect
356 of convective environments on the probability distribution of casualty counts.

357 A tornado-count model like the one demonstrated here could assist forecast guidance (eventually)
358 given a convective outlook that highlights an area of elevated risk for tornadoes and a forecast of
359 CAPE and shear across the elevated-risk area. The statistical model would need to be calibrated to
360 predicted areas and predicted environmental values, but the same model equation used here will
361 provide a probability distribution on the number of tornadoes that should retain some level of skill.

362 Further, a numerical convolution of this probability distribution with a probability distribution
363 for each EF-rating category (Elsner and Schroder 2019) will give a forecast of the expected number
364 of counts by category as well as the associated uncertainties. Output from a model that estimates

365 the number of tornadoes together with output from the cumulative logistic model provides a
366 prediction for the expected number of tornadoes by each EF category. Suppose for example that
367 given current environmental conditions a model predicts the distribution for the total number of
368 tornadoes centered on fifteen while the cumulative logistic regression model predicts that for each
369 tornado there is a fifty percent chance of it being EF0, a ten percent chance of it being EF1, a five
370 percent chance of it being EF2, and so on. Then a numerical convolution of these two distributions
371 provides an expected number of counts by EF rating as well as the associated uncertainties.

372 Similarly, the casualty-count model might prove useful for communicating the risk given the
373 population within the elevated risk area. Of course, first it would be necessary to fit the model to
374 null cases where conditions are forecast to be favorable for an outbreak of tornadoes but only a few
375 (or none) occur consistent with other research (Mercer et al. 2012; Shafer et al. 2009). A separate
376 model (e.g., logistic regression) that predicts the probability that the outbreak will contain at least
377 ten tornadoes could be developed.

378 A casualty-count model can also be employed in a research setting to help better understand the
379 socioeconomic, demographic, and communication factors that make some communities particularly
380 vulnerable to deaths and injuries (Dixon and Moore 2012; Senkbeil et al. 2013; Klockow et al.
381 2014; Fricker and Elsner 2019). Work along this line has been done at the individual tornado
382 level by identifying unusually devastating events (Fricker and Elsner 2019), but scaling this type
383 of analysis to the cluster-level to identify unusually devastating outbreaks might provide additional
384 insights.

385 Finally, it is possible that the models could be improved by including nonlinear effects. One
386 type of non-linearity is interaction where the effect of CAPE on casualties is modulated by shear,
387 for example. However, interaction effects usually must be specified without reference to the data,
388 so additional research on this is needed. The models also might be improved by adjusting the

389 threshold definition of a cluster. Increasing the threshold on the tornado-count model from 10 to
390 14 decreases the sample size to 505 clusters and reduces the effect sizes on CAPE and shear by
391 around 25%. Decreasing the threshold from 10 to 6 increases the sample size and, thus, reduces
392 the standard error assuming the effect size stays the same. A casualty-count model might also be
393 improved by relaxing the assumption that the numbers of people injured or killed are independent.
394 Casualty counts are typically not independent at the household level where multiple people live
395 under the same roof. In this case a better probability model for the data might be a zero-inflated
396 count process rather than a negative binomial process.

397 *Acknowledgments.* The negative binomial regression models in this paper were implemented with
398 the `glm.nb` function from the MASS R package (Venables and Ripley 2002). Graphics were made
399 with the `ggplot2` framework (Wickham 2017). The code and data to fit all the models is available
400 on GitHub (<https://github.com/jelsner/cape-shear>).

References

- Allen, J. T., M. K. Tippett, and A. H. Sobel, 2015a: An empirical model relating U.S. monthly hail occurrence to large-scale meteorological environment. *Journal of Advances in Modeling Earth Systems*, **7** (1), 226–243, doi:10.1002/2014MS000397, URL <https://agupubs.onlinelibrary.wiley.com/doi/abs/10.1002/2014MS000397>.
- Allen, J. T., M. K. Tippett, and A. H. Sobel, 2015b: Influence of the El Niño/Southern Oscillation on tornado and hail frequency in the United States. *Nature Geosciences*, **8**, 278–283.
- Anderson-Frey, A. K., and H. Brooks, 2019: Tornado fatalities: An environmental perspective. *Weather and Forecasting*, **34** (6), 1999–2015, doi:10.1175/waf-d-19-0119.1, URL <https://doi.org/10.1175/waf-d-19-0119.1>.
- Ashley, W. S., and S. M. Strader, 2016: Recipe for disaster: How the dynamic ingredients of risk and exposure are changing the tornado disaster landscape. *Bulletin of the American Meteorological Society*, **97**, 767–786.
- Brooks, H. E., G. W. Carbin, and P. T. Marsh, 2014: Increased variability of tornado occurrence in the United States. *Science*, **346** (6207), 349–352, doi:10.1126/science.1257460, URL <https://science.sciencemag.org/content/346/6207/349>, <https://science.sciencemag.org/content/346/6207/349.full.pdf>.
- Brooks, H. E., C. A. Doswell , and J. Cooper, 1994: On the environments of tornadic and nontornadic mesocyclones. *Weather and Forecasting*, **9**, 606–618, doi:10.1175/1520-0434.
- Cohen, A. E., J. B. Cohen, R. L. Thompson, and B. T. Smith, 2018: Simulating tornado probability and tornado wind speed based on statistical models. *Weather and Forecasting*, **33** (4), 1099–1108, doi:10.1175/waf-d-17-0170.1, URL <https://doi.org/10.1175/waf-d-17-0170.1>.

- 423 Concannon, P., H. E. Brooks, and C. A. Doswell , 2000: Climatological risk of strong and violent
424 tornadoes in the United States. *Second Conference on Environmental Applications*.
- 425 Dean, A. R., 2010: P2.19 An analysis of clustered tornado events. *25th Conference on Severe Local*
426 *Storms*.
- 427 Dixon, P. G., A. E. Mercer, K. Grala, and W. H. Cooke, 2014: Objective identification of tornado
428 seasons and ideal spatial smoothing radii. *Earth Interactions*, **18**, 1–15.
- 429 Dixon, R. W., and T. W. Moore, 2012: Tornado vulnerability in Texas. *Weather, Climate, and*
430 *Society*, **4**, 59–68.
- 431 Doswell, C. A., R. Edwards, R. L. Thompson, J. A. Hart, and K. C. Crosbie, 2006: A simple and
432 flexible method for ranking severe weather events. *Weather and Forecasting*, **21 (6)**, 939–951,
433 doi:10.1175/waf959.1, URL <https://doi.org/10.1175/waf959.1>.
- 434 Elsner, J. B., S. C. Elsner, and T. H. Jagger, 2015: The increasing efficiency of tornado days in the
435 United States. *Climate Dynamics*, **45 (3-4)**, 651–659.
- 436 Elsner, J. B., T. Fricker, and W. D. Berry, 2018: A model for U.S. tornado casualties involving
437 interaction between damage path estimates of population density and energy dissipation. *Journal*
438 *of Applied Meteorology and Climatology*, **57**, 2035–2046.
- 439 Elsner, J. B., and C. P. Schertmann, 1994: Assessing forecast skill through cross validation.
440 *Weather and Forecasting*, **9 (4)**, 619–624.
- 441 Elsner, J. B., and Z. Schroder, 2019: Tornado damage ratings estimated with cumulative logistic
442 regression. *Journal of Applied Meteorology and Climatology*, **58 (12)**, 2733–2741, doi:10.1175/
443 jamc-d-19-0178.1, URL <https://doi.org/10.1175/jamc-d-19-0178.1>.

444 Fricker, T., and J. B. Elsner, 2019: Unusually devastating tornadoes in the United States:
445 1995–2016. *Annals of the American Association of Geographers*, **110** (3), 724–738, doi:
446 10.1080/24694452.2019.1638753, URL <https://doi.org/10.1080/24694452.2019.1638753>.

447 Fricker, T., J. B. Elsner, and T. H. Jagger, 2017: Population and energy elasticity of tornado
448 casualties. *Geophysical Research Letters*, **44**, 3941–3949, doi:10.1002/2017GL073093.

449 Fujita, T. T., 1981: Tornadoes and downbursts in the context of generalized planetary scales. *J.*
450 *Atmos. Sci.*, **38**, 1511–1534.

451 Gensini, V., and W. Ashley, 2011: Climatology of potentially severe convective environments from
452 the North American Regional Reanalysis. *Electronic Journal of Severe Storms Meteorology*, **6**,
453 1–40, doi:10.1038/s41612-018-0048-2.

454 Gensini, V. A., T. L. Mote, and H. E. Brooks, 2014: Severe-thunderstorm reanalysis environments
455 and collocated radiosonde observations. *Journal of Applied Meteorology and Climatology*,
456 **53** (3), 742–751, doi:10.1175/jamc-d-13-0263.1, URL <https://doi.org/10.1175/jamc-d-13-0263.1>.

457 1.

458 Heiss, W. H., D. L. McGrew, and D. Sirmans, 1990: NEXRAD: next generation weather radar
459 (WSR-88D). *Microwave Journal*, **33** (1), 79.

460 Hilbe, J., 2011: *Negative Binomial Regression*. Cambridge University Press.

461 Hill, A. J., G. R. Herman, and R. S. Schumacher, 2020: Forecasting severe weather with random
462 forests. *Monthly Weather Review*, doi:10.1175/mwr-d-19-0344.1, URL <https://doi.org/10.1175/mwr-d-19-0344.1>.

463 mwr-d-19-0344.1.

464 Hitchens, N. M., and H. E. Brooks, 2014: Evaluation of the Storm Prediction Center's convective
465 outlooks from day 3 through day 1. *Weather and Forecasting*, **29** (5), 1134–1142, doi:10.1175/
466 waf-d-13-00132.1, URL <https://doi.org/10.1175/waf-d-13-00132.1>.

467 Jackson, J. D., and M. E. Brown, 2009: Sounding-derived low-level thermodynamic characteristics
468 associated with tornadic and non-tornadic supercell environments in the Southeast United States.
469 *National Weather Digest*, **33**, 16–26.

470 Klockow, K. E., R. A. Pepler, and R. A. McPherson, 2014: Tornado folk science in Alabama
471 and Mississippi in the 27 April 2011 tornado outbreak. *GeoJournal*, **79** (6), 791–804, doi:
472 10.1007/s10708-013-9518-6, URL <https://doi.org/10.1007/s10708-013-9518-6>.

473 Mercer, A. E., C. M. Shafer, C. A. Doswell, L. M. Leslie, and M. B. Richman, 2012: Synoptic
474 composites of tornadic and nontornadic outbreaks. *Monthly Weather Review*, **140** (8), 2590–
475 2608, doi:10.1175/mwr-d-12-00029.1, URL <https://doi.org/10.1175/mwr-d-12-00029.1>.

476 Mesinger, F., and Coauthors, 2006: North American Regional Reanalysis. *Bulletin of the American*
477 *Meteorological Society*, **87** (3), 343–360, doi:10.1175/BAMS-87-3-343, URL <https://doi.org/10.1175/BAMS-87-3-343>,
478 <https://doi.org/10.1175/BAMS-87-3-343>.

479 Moore, T., 2017: On the temporal and spatial characteristics of tornado days in the United States.
480 *Atmospheric Research*, **184**, doi:10.1016/j.atmosres.2016.10.007.

481 Moore, T. W., R. W. Dixon, and N. J. Sokol, 2016: Tropical cyclone Ivan's tornado cluster
482 in the Mid-Atlantic region of the United States on 17–18 September 2004. *Physical Geogra-*
483 *phy*, **37** (3-4), 210–227, doi:10.1080/02723646.2016.1189299, URL [https://doi.org/10.1080/](https://doi.org/10.1080/02723646.2016.1189299)
484 [02723646.2016.1189299](https://doi.org/10.1080/02723646.2016.1189299).

485 Rasmussen, E. N., and D. O. Blanchard, 1998: A baseline climatology of sounding-
486 derived supercell and tornado forecast parameters. *Weather and Forecasting*, **13** (4), 1148–
487 1164, doi:10.1175/1520-0434(1998)013<1148:ABCOSD>2.0.CO;2, URL [https://doi.org/10.1175/1520-0434\(1998\)013<1148:ABCOSD>2.0.CO;2](https://doi.org/10.1175/1520-0434(1998)013<1148:ABCOSD>2.0.CO;2).

489 Schroder, Z., and J. B. Elsner, 2019: Quantifying relationships between environmental factors
490 and power dissipation on the most prolific days in the largest tornado “outbreaks”. *International*
491 *Journal of Climatology*, doi:10.1002/joc.6388, URL <https://doi.org/10.1002/joc.6388>.

492 Senkbeil, J. C., D. A. Scott, P. Guinazu-Walker, and M. S. Rockman, 2013: Ethnic and racial
493 differences in tornado hazard perception, preparedness, and shelter lead time in Tuscaloosa. *The*
494 *Professional Geographer*, **66** (4), 610–620, doi:10.1080/00330124.2013.826562, URL <https://doi.org/10.1080/00330124.2013.826562>.

496 Shafer, C. M., and C. A. Doswell, 2011: Using kernel density estimation to identify, rank, and
497 classify severe weather outbreak events. *Electronic Journal of Severe Storms Meteorology*, **6**,
498 1–28.

499 Shafer, C. M., A. E. Mercer, C. A. Doswell, M. B. Richman, and L. M. Leslie, 2009: Evaluation
500 of WRF forecasts of tornadic and nontornadic outbreaks when initialized with synoptic-scale
501 input. *Monthly Weather Review*, **137** (4), 1250–1271, doi:10.1175/2008mwr2597.1, URL <https://doi.org/10.1175/2008mwr2597.1>.

503 Steiner, E., 2019: Spatial history project. Center for Spatial and Textual Analysis, Stanford Uni-
504 versity, URL <http://web.stanford.edu/group/spatialhistory/cgi-bin/site/index.php>.

505 Thompson, R. L., R. Edwards, J. A. Hart, K. L. Elmore, and P. Markowski, 2003: Close proxim-
506 ity soundings within supercell environments obtained from the Rapid Update Cycle. *Weather*

507 *and Forecasting*, **18 (6)**, 1243–1261, doi:10.1175/1520-0434(2003)018<1243:cpswse>2.0.co;2,
508 URL [https://doi.org/10.1175/1520-0434\(2003\)018<1243:cpswse>2.0.co;2](https://doi.org/10.1175/1520-0434(2003)018<1243:cpswse>2.0.co;2).

509 Thompson, R. L., and Coauthors, 2017: Tornado damage rating probabilities derived from WSR-
510 88D data. *Weather and Forecasting*, **32 (4)**, 1509–1528, doi:10.1175/waf-d-17-0004.1, URL
511 <https://doi.org/10.1175/waf-d-17-0004.1>.

512 Tippett, M. K., C. Lepore, and J. E. Cohen, 2016: More tornadoes in the most extreme U.S.
513 tornado outbreaks. *Science*, **354 (6318)**, 1419–1423, doi:10.1126/science.aah7393, URL <https://doi.org/10.1126/science.aah7393>.
514

515 Tippett, M. K., A. H. Sobel, and S. J. Camargo, 2012: Association of U.S. tornado occurrence
516 with monthly environmental parameters. *Geophysical Research Letters*, **39**, L02 801.

517 Venables, W. N., and B. D. Ripley, 2002: *Modern Applied Statistics with S*. 4th ed., Springer, New
518 York, URL <http://www.stats.ox.ac.uk/pub/MASS4>, ISBN 0-387-95457-0.

519 Wickham, H., 2017: *tidyverse: Easily Install and Load 'Tidyverse' Packages*. URL [https://CRAN.](https://CRAN.R-project.org/package=tidyverse)
520 [R-project.org/package=tidyverse](https://CRAN.R-project.org/package=tidyverse), r package version 1.1.1.

521 **LIST OF TABLES**

522 **Table 1.** Cluster statistics by time of day. Each cluster is categorized by the closest
523 three-hour time (defined by the NARR data) prior to the first tornado. 26

524 **Table 2.** Correlation matrix of environmental variables considered in this study. Dew-
525 point temperature (DEW), specific humidity (SH), and storm relative helicity
526 (HLCY). Only CAPE, CIN, DLBS, and SLBS are used as explanatory variables
527 in the models. 27

528 **Table 3.** Variables considered in the regression models. Values include the range and
529 average across the 768 tornado clusters. 28

530 **Table 4.** Coefficients in the tornado-count models. The size parameter (n) is $6.27 \pm .393$
531 (standard error) for the initial model $6.25 \pm .392$ (standard error) for the final
532 model. 29

533 **Table 5.** Coefficients in the casualty-county models. The size parameter (n) is $.261 \pm .014$
534 (standard error) for the initial and final models. 30

535 TABLE 1. Cluster statistics by time of day. Each cluster is categorized by the closest three-hour time (defined
 536 by the NARR data) prior to the first tornado.

Time of Day (UTC)	Number of Clusters	Number of Tornadoes	Tornadoes Per Cluster	Average Duration (hours)
00	33	523	15.8	6.1
03	5	67	13.4	6.4
06	2	23	11.5	3.2
12	145	3598	12.1	14.0
15	124	3222	26.0	11.5
18	249	5220	21.0	8.4
21	210	4416	21.0	7.0

537 TABLE 2. Correlation matrix of environmental variables considered in this study. Dew-point temperature
 538 (DEW), specific humidity (SH), and storm relative helicity (HLCY). Only CAPE, CIN, DLBS, and SLBS are
 539 used as explanatory variables in the models.

	CAPE	CIN	DLBS	SLBS	HLCY	DEW	SH
CAPE	1.00						
CIN	-0.07	1.00					
DLBS	-0.03	-0.29	1.00				
SLBS	-0.37	-0.24	0.49	1.00			
HLCY	-0.22	-0.30	0.58	0.76	1.00		
DEW	0.56	0.00	-0.08	0.02	-0.08	1.00	
SH	0.64	0.00	-0.12	-0.08	-0.13	0.98	1.00

540 TABLE 3. Variables considered in the regression models. Values include the range and average across the 768
 541 tornado clusters.

Variable	Abbreviation	Range	Average
Explanatory Variables			
Convective Available Potential Energy [J kg^{-1}]	CAPE	[0, 6530]	2225
Convective Inhibition [J kg^{-1}]	CIN	[-668, 0]	-114
Deep-Layer Bulk Shear [m s^{-1}]	DLBS	[5.6, 48]	27.5
Shallow-Layer Bulk Shear [m s^{-1}]	SLBS	[1.1, 33.8]	15.0
Latitude [$^{\circ}$ N]	ϕ	[27.12, 48.97]	37.20
Longitude [$^{\circ}$ E]	λ	[-109.9 -72.88]	-92.16
Cluster Area [km^2]	A	[361, 1 064 337]	167 990
Population [No. of People]	P	[0, 38 226 946]	3 387 259
Year	Y	[1994, 2018]	2006
Response Variables			
Number of Tornadoes	T	[0, 173]	22.2
Number of Casualties (injuries plus deaths)	C	[0, 3 069]	29.9

542 TABLE 4. Coefficients in the tornado-count models. The size parameter (n) is $6.27 \pm .393$ (standard error) for
 543 the initial model $6.25 \pm .392$ (standard error) for the final model.

Coefficient	Estimate	S.E.	z value	$\Pr(> z)$
Initial Model				
β_0	4.5489	4.7662	0.9540	0.3399
β_A	0.0146	0.0011	12.80	< 0.0001
β_ϕ	-0.0051	0.0043	-1.17	0.2427
β_λ	-0.0028	0.0031	-0.917	0.3594
β_Y	-0.0012	0.0024	-0.515	0.6068
β_{CAPE}	0.0452	0.0153	2.96	0.0031
β_{CIN}	-0.0110	0.0189	-0.581	0.5612
β_{DLBS}	0.1256	0.0292	4.30	< 0.0001
β_{SLBS}	0.1059	0.0355	2.98	0.0029
Final Model				
β_0	2.1779	0.0817	26.65	< 0.0001
β_A	0.0149	0.0011	13.85	< 0.0001
β_{CAPE}	0.0459	0.0146	3.13	0.0017
β_{DLBS}	0.1254	0.0288	4.35	< 0.0001
β_{SLBS}	0.1054	0.0314	3.35	0.0008

544 TABLE 5. Coefficients in the casualty-county models. The size parameter (n) is $.261 \pm .014$ (standard error)
 545 for the initial and final models.

Coefficient	Estimate	S.E.	z value	$\Pr(> z)$
Initial Model				
β_0	76.6908	20.7430	3.70	0.0002
β_P	0.0122	0.0019	6.51	< 0.0001
β_ϕ	-0.0561	0.0187	-3.00	0.0027
β_λ	0.0284	0.0136	2.09	0.0363
β_Y	-0.0364	0.0103	-3.52	0.0004
β_{CAPE}	0.2436	0.0643	3.79	0.0002
β_{CIN}	0.0052	0.0802	0.07	0.9479
β_{DLBS}	0.6853	0.1262	5.43	< 0.0001
β_{SLBS}	0.5650	0.1534	3.68	0.0002
Final Model				
β_0	76.7677	20.6902	3.71	0.0002
β_P	0.0122	0.0018	6.67	0.0000
β_ϕ	-0.0563	0.0186	-3.02	0.0025
β_λ	0.0287	0.0130	2.20	0.0277
β_Y	-0.0364	0.0103	-3.53	0.0004
β_{CAPE}	0.2440	0.0643	3.79	0.0001
β_{DLBS}	0.6833	0.1253	5.45	0.0000
β_{SLBS}	0.5631	0.1504	3.74	0.0002

546 **LIST OF FIGURES**

547 **Fig. 1.** Example tornado clusters. Each point is the tornadogenesis location shaded by EF rating.
 548 The black line is the spatial extent of the tornadoes occurring on that convective day and is
 549 defined by the minimum convex hull encompassing the set of locations. 32

550 **Fig. 2.** Histograms of the number of clusters by number of tornadoes (A) and number of clusters by
 551 number of casualties (B). The histograms are right-truncated at 50 to show detail on the left
 552 side of the distributions. Only clusters with at least ten tornadoes are considered in this study. . . 33

553 **Fig. 3.** Probability of a cluster (A), average number of tornadoes per cluster (B), and average number
 554 of casualties per 100 000 people per cluster (C) by week of the year. 34

555 **Fig. 4.** Observed cluster-level tornado counts versus predicted rates from a negative binomial re-
 556 gression. The thin black line is the line of best fit. The thick line is the slope of the
 557 model indicating the relationship between the observed and predicted tornado counts and the
 558 associated standard error. 35

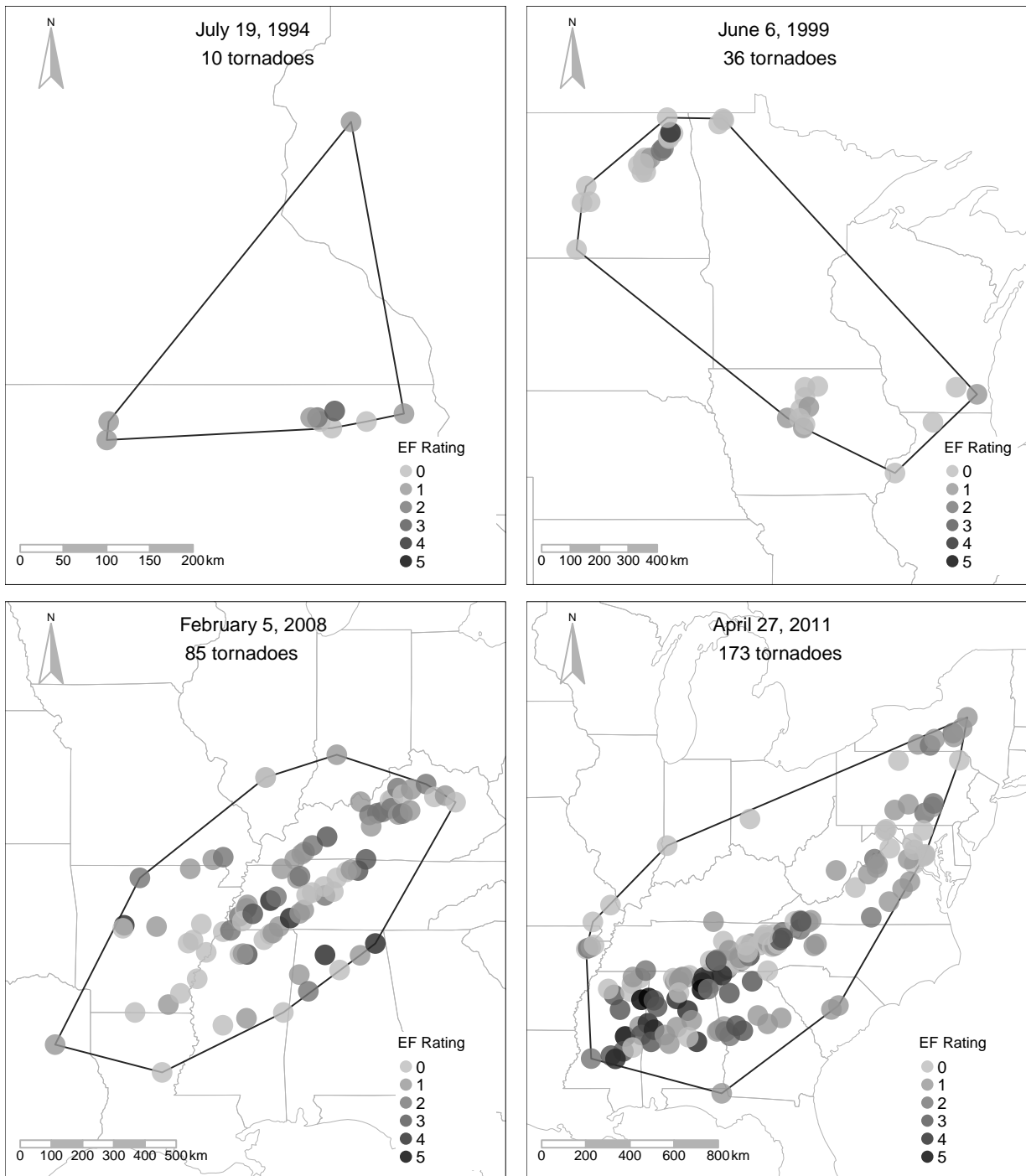
559 **Fig. 5.** Estimated probability of at least 30 tornadoes given an outbreak of at least ten tornadoes
 560 and the regression model. The predicted count from the model is a parameter in a negative
 561 binomial distribution with cluster area set at 400 000 km² and shallow-level bulk shear is set
 562 to its mean value. 36

563 **Fig. 6.** Estimated probability of at least 30 tornadoes given an outbreak of at least ten tornadoes and
 564 the regression model across a range of CAPE and deep-layer bulk shear values holding the
 565 shallow-layer bulk shear at a mean value. 37

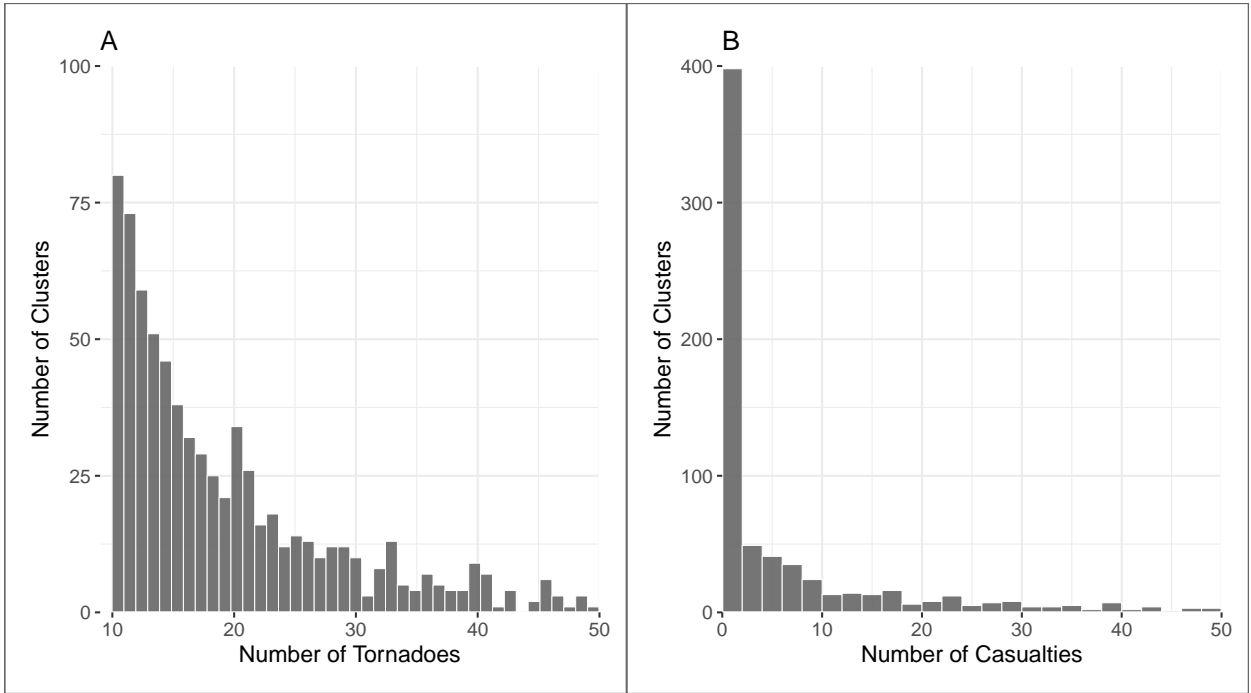
566 **Fig. 7.** Observed cluster-level casualty counts versus predicted rates from a negative binomial re-
 567 gression. Clusters without casualties are plotted at the far left. The thin black line is the line
 568 of best fit. The thick line is the slope of the model indicating the relationship between the
 569 observed and predicted tornado counts and the associated standard error. 38

570 **Fig. 8.** Probability of at least 50 tornado casualties as a function of deep-layer bulk shear and CAPE
 571 and modulated by the number of people in harm’s way. The other variables are set at their
 572 mean values and year is set at 2018. 39

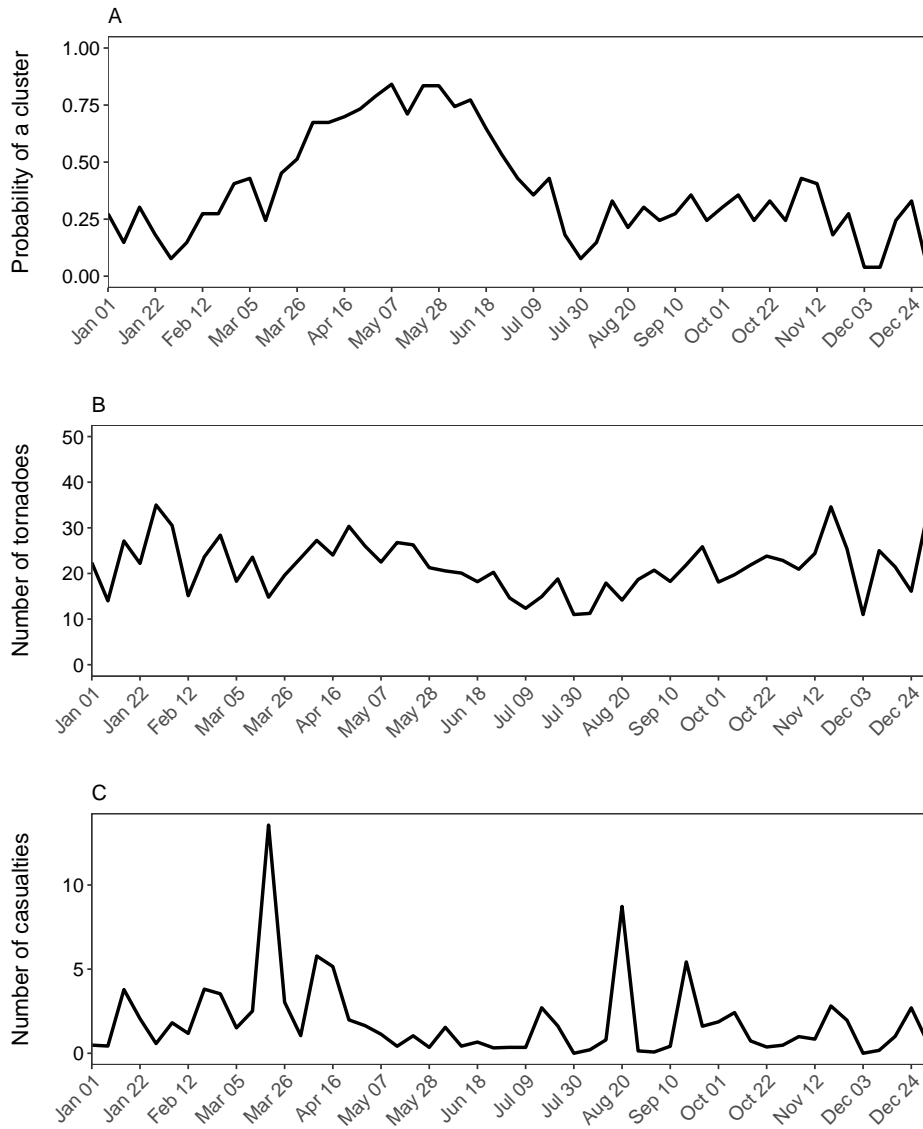
573 **Fig. 9.** Probability of at least 25 tornado casualties as a function of deep-layer bulk shear and CAPE
 574 and modulated by location for two *hypothetical* outbreaks, one centered over Sioux City,
 575 Iowa, and the other centered over Birmingham, Alabama. The shallow-layer bulk shear is
 576 set to its mean value, year is set to 2018, and population is set to 4M. 40



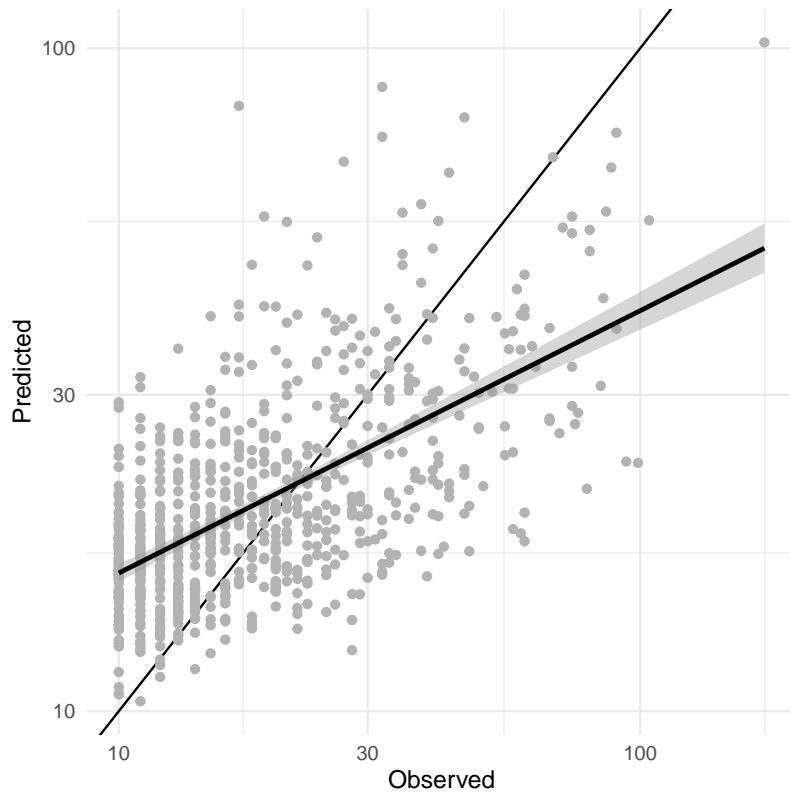
577 FIG. 1. Example tornado clusters. Each point is the tornadogenesis location shaded by EF rating. The black
 578 line is the spatial extent of the tornadoes occurring on that convective day and is defined by the minimum convex
 579 hull encompassing the set of locations.



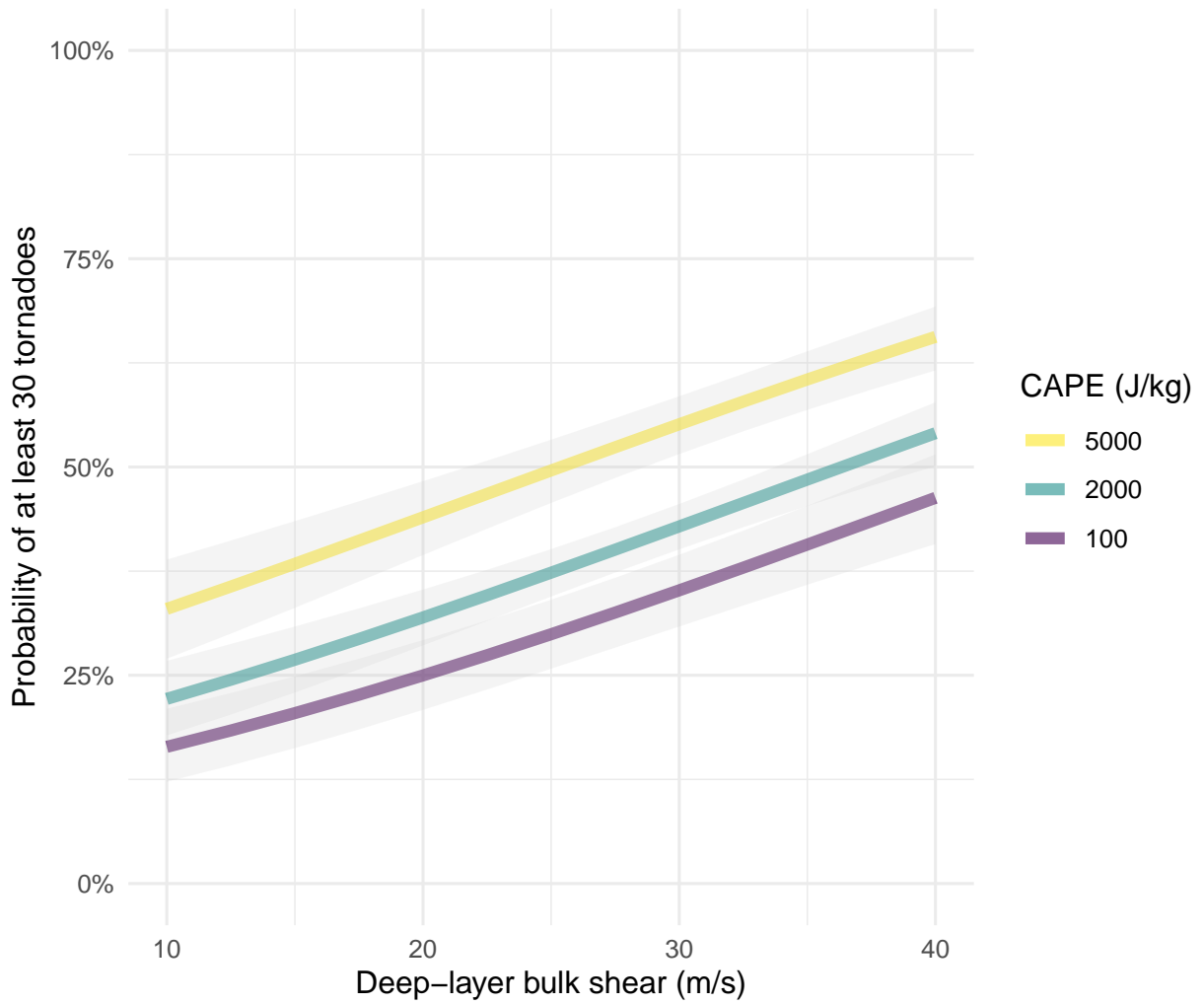
580 FIG. 2. Histograms of the number of clusters by number of tornadoes (A) and number of clusters by number of
 581 casualties (B). The histograms are right-truncated at 50 to show detail on the left side of the distributions. Only
 582 clusters with at least ten tornadoes are considered in this study.



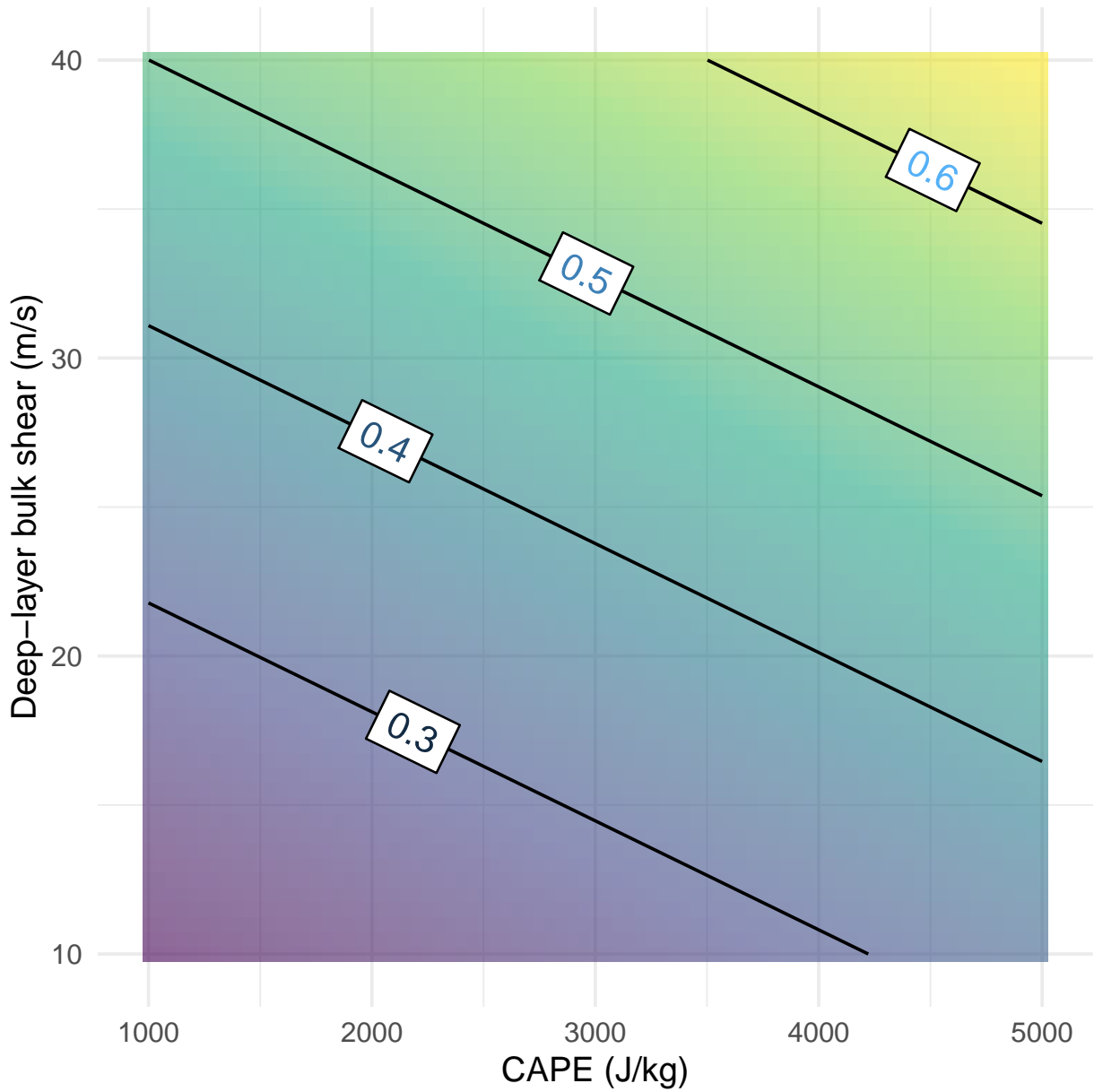
583 FIG. 3. Probability of a cluster (A), average number of tornadoes per cluster (B), and average number of
 584 casualties per 100 000 people per cluster (C) by week of the year.



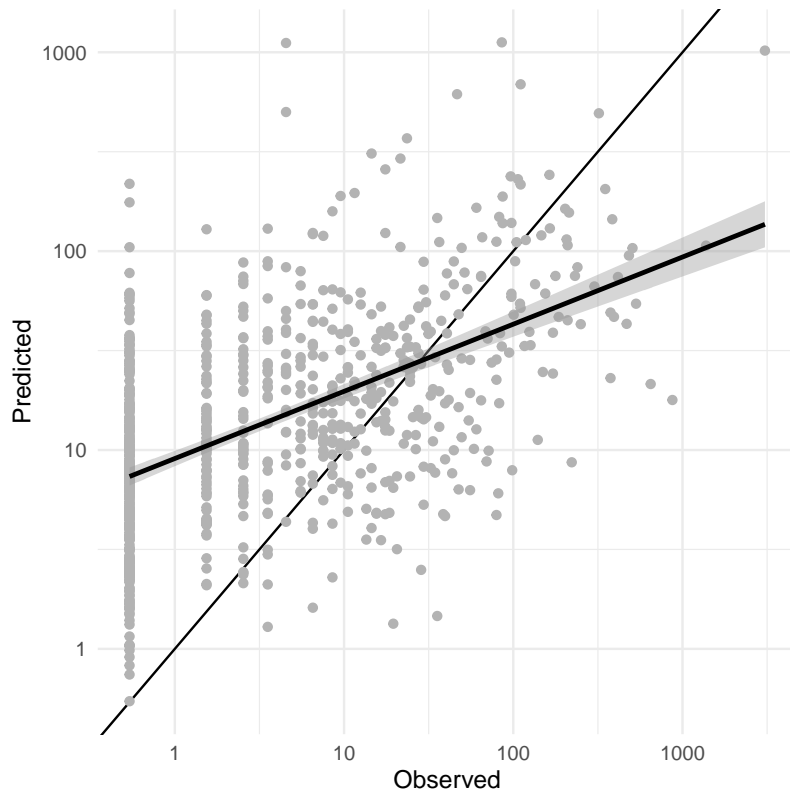
585 FIG. 4. Observed cluster-level tornado counts versus predicted rates from a negative binomial regression. The
586 thin black line is the line of best fit. The thick line is the slope of the model indicating the relationship between
587 the observed and predicted tornado counts and the associated standard error.



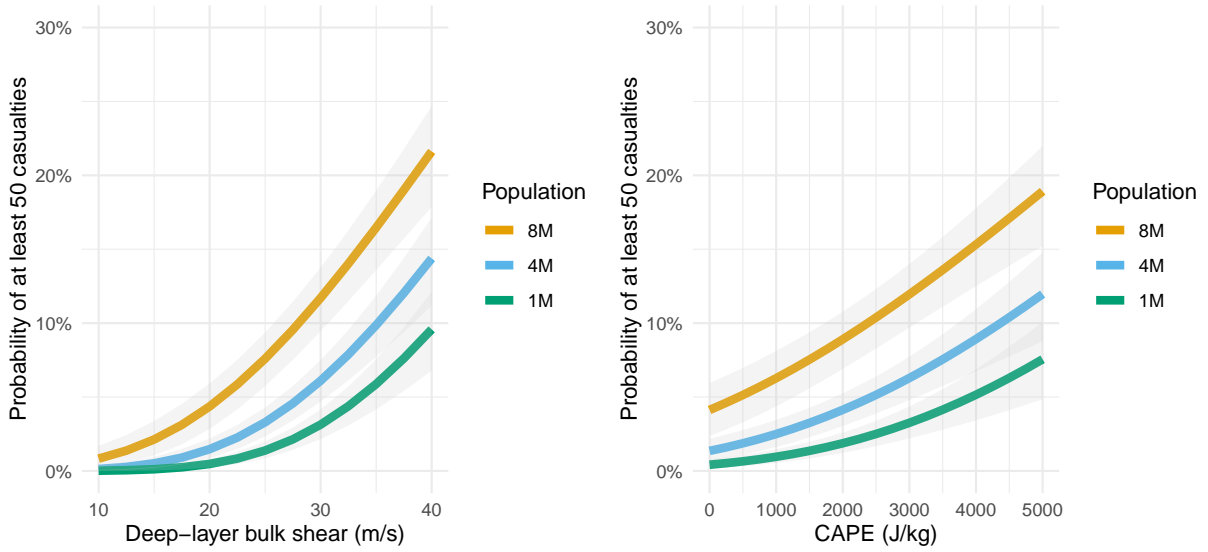
588 FIG. 5. Estimated probability of at least 30 tornadoes given an outbreak of at least ten tornadoes and the
 589 regression model. The predicted count from the model is a parameter in a negative binomial distribution with
 590 cluster area set at 400 000 km² and shallow-level bulk shear is set to its mean value.



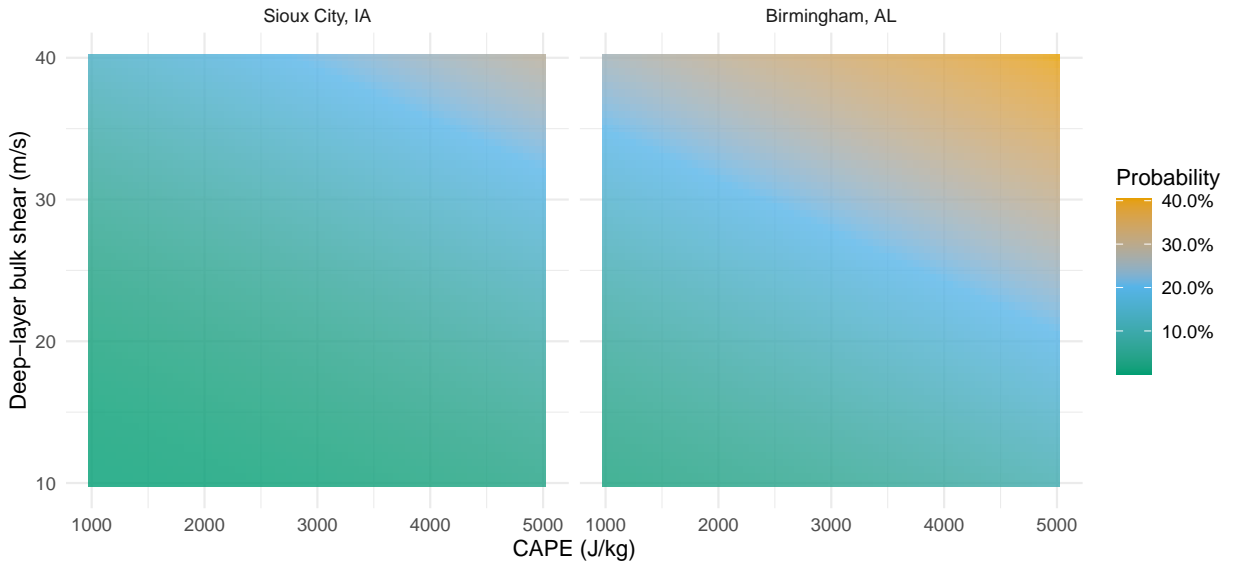
591 FIG. 6. Estimated probability of at least 30 tornadoes given an outbreak of at least ten tornadoes and the
 592 regression model across a range of CAPE and deep-layer bulk shear values holding the shallow-layer bulk shear
 593 at a mean value.



594 FIG. 7. Observed cluster-level casualty counts versus predicted rates from a negative binomial regression.
595 Clusters without casualties are plotted at the far left. The thin black line is the line of best fit. The thick line
596 is the slope of the model indicating the relationship between the observed and predicted tornado counts and the
597 associated standard error.



598 FIG. 8. Probability of at least 50 tornado casualties as a function of deep-layer bulk shear and CAPE and
 599 modulated by the number of people in harm's way. The other variables are set at their mean values and year is
 600 set at 2018.



601 FIG. 9. Probability of at least 25 tornado casualties as a function of deep-layer bulk shear and
 602 modulated by location for two *hypothetical* outbreaks, one centered over Sioux City, Iowa, and the other centered
 603 over Birmingham, Alabama. The shallow-layer bulk shear is set to its mean value, year is set to 2018, and
 604 population is set to 4M.